ON THE PERFORMANCE OF MULTI-H CPM IN MULTIPATH INTERFERENCE

Erik Perrins
Department of Electrical and Computer Engineering
Brigham Young University
Provo, UT 84602
esp@ee.byu.edu

Faculty Advisor:
Michael Rice

ABSTRACT

The performance of multi-h CPM over multipath interference channels is evaluated with computer simulations using the optimal coherent receiver and a suboptimal noncoherent receiver. For channels with high-amplitude short-delay multipath reflections, the simulations show that both receivers reach an error floor in their performance as the amplitude of the multipath reflections grows. The rate of degradation for the noncoherent receiver is worse than for the coherent receiver. For channels with low-amplitude long-delay reflections the coherent and noncoherent receivers had losses of 1 dB and 3 dB respectively relative to their respective unfaded performance.

INTRODUCTION

The Advanced Range Telemetry (ARTM) Tier II waveform is multi-h CPM. Some of the attractive features of this modulation format are that it has constant envelope and narrow bandwidth [1]. The ARTM Tier II CPM variant has a 4-ary symbol alphabet, it uses a raised cosine frequency pulse spanning 3 symbol intervals, and has modulation indices $4/16$ and $5/16$. A challenge facing the receiver in most instances is multipath interference. The objective of this work is to evaluate the performance of the ARTM Tier II waveform over a multipath channel where the received signal consists of a direct component, a multipath component, and additive noise, modeled by

$$r(t) = \underbrace{s(t)}_{\text{direct component}} + \underbrace{\Gamma s(t-\tau)}_{\text{multipath component}} + \underbrace{n(t)}_{\text{noise}}. \tag{1}$$

In Equation (1), $s(t)$ is the transmitted signal and $r(t)$ is the received signal. The multipath component is delayed by τ seconds and attenuated by the complex-valued reflection coefficient Γ. The physics of the model imply that the reflected signal is weaker than the original signal. This in turn implies that the magnitude of Γ is less than unity [2, 3, 4]. Two special cases of this channel are considered in this work. The first is where the delay is short relative to the symbol interval T (i.e. $\tau < T$), and the multipath reflection is strong (i.e. Γ is close to unity). The second is where the delay is long, perhaps several multiples of T, and the reflection is weak, $\Gamma \leq 0.1$.

The ARTM Tier II waveform is simulated over these two channels using the optimum coherent maximum likelihood sequence estimating (MLSE) receiver presented in [5], and the suboptimal noncoherent sequence estimating (NCSE) receiver presented in [6]. The NCSE receiver has a filter which introduces an additional L_F symbols of intersymbol interference (ISI). This is above and beyond the ISI introduced by the CPM modulation. To account for this, the NCSE receiver has a design parameter $L'_F \leq L_F$ which determines the size of the demodulator's trellis and ultimately the receiver complexity. By allowing L'_F to be less than L_F, the receiver can ignore this additional ISI to some degree and have reduced complexity at the expense of performance. In this case $L'_F = L_F = 1$. The receiver is referred to as NCSE(1). The simulation results for these two channel cases are presented in the following two sections.

STRONG REFLECTION SHORT-DELAY

The first channel case is referred to as the strong-short channel. The model for the reflection coefficient is $\Gamma = |\Gamma|e^{j\phi}$. The phase ϕ determines the location of the null in the channel response [2, 3, 4]. The magnitude of Γ determines how deep the null is. This is shown in Figure 1. In the Figure, the delay is $\tau = 0.2T$ and the reflection coefficient is $\Gamma = 0.9e^{-j0.85\pi}$, where the phase was set to -0.85π to position the null just above carrier frequency.

The performance of the ARTM Tier II multi-h waveform was simulated over this channel with $|\Gamma|$ ranging from small to large, $|\Gamma| = 0.1, 0.2, \cdots, 0.9$. The weaker values of $|\Gamma|$ are included in the simulation to show what happens as $|\Gamma|$ increases. The nine performance curves (one for each increasing value of $|\Gamma|$) are shown for both receivers in Figure 2. The curves show that the receiver performance is significantly degraded as $|\Gamma|$ increases. For the MLSE receiver, the curves for $|\Gamma| = 0.1, 0.2, 0.3,$ and 0.4 (the four smallest values) are closely grouped together as seen in Figure 2 a). The curves for the four largest values of $|\Gamma|$ ($0.6, 0.7, 0.8,$ and 0.9) are also closely grouped together with a considerable distance between the two groups. The $|\Gamma| = 0.5$ curve is separate from both groups. The degradation is especially bad considering that each of the four curves in the large $|\Gamma|$ group reaches its own error floor in which the BER does not go to zero as E_b/N_0 goes to infinity. There are also several anomalies in this group of curves. In particular, the $|\Gamma| = 0.6$ curve flattens out and actually performs worse than the $|\Gamma| = 0.7$ curve at the higher values of E_b/N_0. This particular combination of magnitude and phase for the reflection coefficient have a particularly strong effect on the phase trellis of the signal. This causes different paths through the trellis to be more easily confused with one another resulting in more errors.

The set of curves for the NCSE(1) receiver are shown in Figure 2 b). They are somewhat different than those for the MLSE case in that they are much more evenly distributed and do not cross over one another.

At BER = 10^{-5}, the NCSE(1) receiver operates at a loss of 6 dB relative to the MLSE receiver for the smaller values of $|\Gamma|$ and increases to 9 dB for $|\Gamma| = 0.5$. The receivers also have different error floors. A simplified version of the noncoherent receiver, called NCSE(0) [6], showed an additional 1 dB loss over the NCSE(1) receiver which is consistent with earlier findings, these curves are not shown here.

Figure 3 shows the performance loss of the two receivers verses increasing $|\Gamma|$. The loss is measured relative to the unfaded performance of the MLSE receiver [6]. The Figure illustrates how large the losses become as $|\Gamma|$ increases, and also how the performance gap between the two receivers grows. As $|\Gamma|$ increases beyond 0.5 the losses become infinite for both receivers.

WEAK REFLECTION LONG-DELAY

The second case considered is the weak-long channel. The effect this type of channel has on the transmitted signal is shown in Figure 4. In the Figure, the delay is $\tau = 2T$ and the reflection coefficient is $\Gamma = 0.1e^{j0.85\pi}$. The channel produces a minor attenuation across much of the bandwidth of the signal.

The ARTM Tier II waveform was simulated over this channel with these same channel parameters. These results are shown in Figure 5. At BER = 10^{-5}, the MLSE receiver suffers a 1 dB loss relative to its unfaded performance. At the same BER level, the NCSE(1) receiver has a degradation of 3 dB relative to its unfaded performance, and 8 dB relative to the faded MLSE performance. . In addition to the $\tau = 2T$ case shown in Figure 5, simulations were also performed for $\tau = 3T$ and $\tau = 4T$. For these longer delays, both receivers had nearly identical performance as the $\tau = 2T$ case. These additional curves are not shown.

DISCUSSION AND CONCLUSIONS

The performance of the ARTM Tier II multi-h CPM waveform was simulated over two multipath interference channels: one with strong multipath reflection and a short delay, and one with weak reflection and a long delay. The simulations included two receivers: the optimal coherent MLSE receiver, and a suboptimal noncoherent receiver.

In the first case, the simulations found that the performance of both receivers was very poor as evidenced by the observed error floor. In addition, the performance gap between the two receivers increased from 6 dB for weaker multipath reflections, to 9 dB for moderate reflections. This increasing gap implies that the noncoherent receiver becomes a less feasible alternative to the MLSE receiver as the multipath reflections grow stronger; BUT, the simulations also assumed that perfect carrier phase information was available for the MLSE receiver, and that perfect symbol timing was available for both receivers. In a practical system, the loss of carrier phase lock under strong multipath interference would disable the MLSE receiver, while the noncoherent receiver could still produce some output. In the second case, the MLSE receiver suffered only a 1 dB loss relative to its best performance, while the noncoherent receiver suffered a 3 dB loss relative to its best performance. This indicates that the MLSE receiver's performance is degraded less by weak multipath reflections with long delay than the performance of the noncoherent receiver.

REFERENCES

[1] M. Geoghegan. Description and performance results for the advanced range telemetry (ARTM) Tier II waveform. In *Proceedings of the International Telemetering Conference*, San Diego, CA, October 2000.

[2] Michael Rice, Adam Davis, and Christian Bettweiser. A wideband channel model for aeronautical telemetry — Part 1: Geometric considerations and experimental configuration. In *Proceedings of the International Telemetering Conference*, San Diego, CA, October 2002.

[3] Michael Rice, Adam Davis, and Christian Bettweiser. A wideband channel model for aeronautical telemetry — Part 2: Modeling results. In *Proceedings of the International Telemetering Conference*, San Diego, CA, October 2002.

[4] Adam Davis. A wideband channel model for aeronautical telemetry. Master's thesis, Brigham Young University, Provo, UT, 2002.

[5] J. B. Anderson, T. Aulin, C-E. Sundberg. *Digital Phase Modulation*. Plenum Press, New York, 1986.

[6] E. Perrins and M. Rice. Comparison of receivers for multi-h CPM. In *Proceedings of the International Telemetering Conference*, San Diego, CA, October 2002.

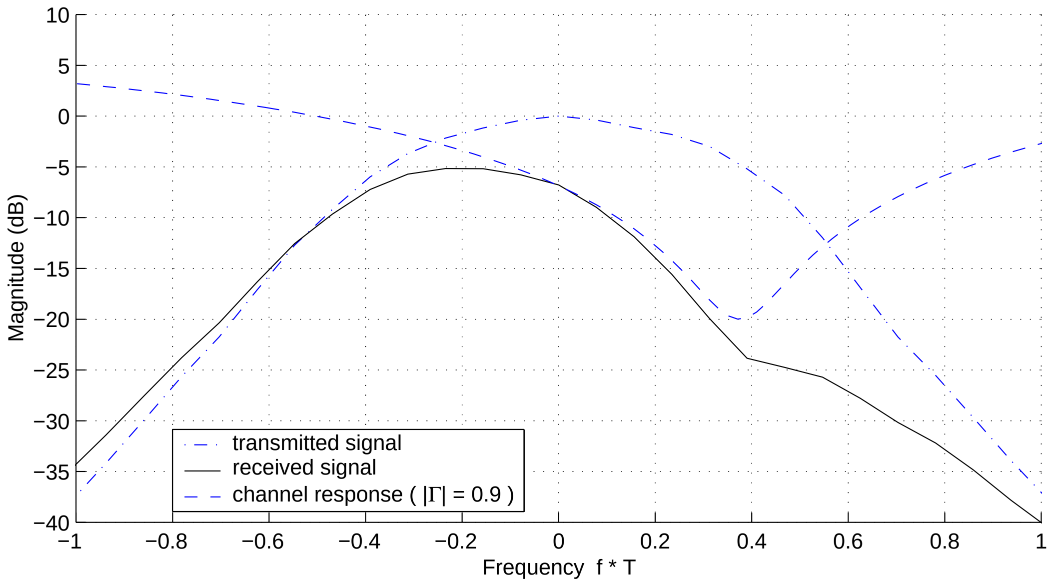

Figure 1: Comparison of multi-h CPM signal before and after passing through the strong-short channel. Channel parameters: $\Gamma = 0.9e^{-j0.85\pi}$, $\tau = 0.2T$. Multi-h parameters: $M = 4$, 3RC with $h = \{4/16, 5/16\}$.

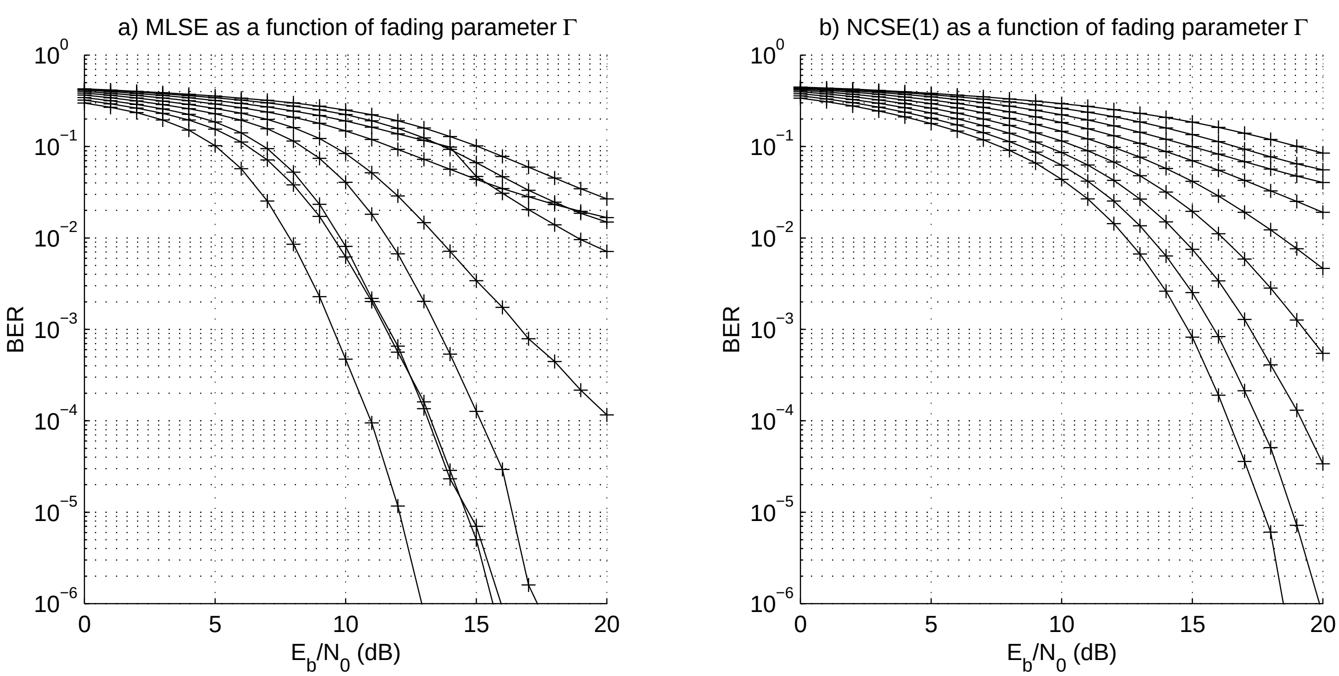

Figure 2: a) Performance of multi-h CPM using MLSE receiver over strong-short channel. The nine curves are for $|\Gamma| = 0.1, 0.2, \cdots, 0.9$. b) Performance using NCSE(1) receiver for same range of $|\Gamma|$. The performance difference between the two receivers at BER = 10^{-5} increases from 6 dB to 9 dB as $|\Gamma|$ increases.

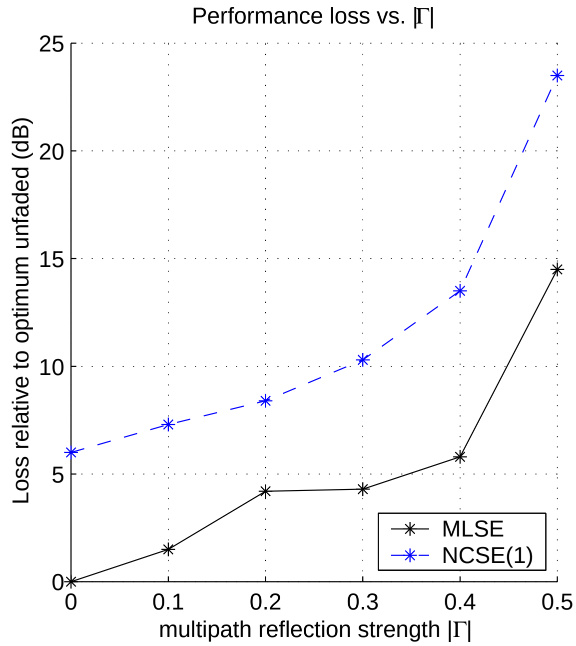

Figure 3: Performance loss of the two receivers vs. multipath reflection strength $|\Gamma|$. The loss is measured relative to the unfaded performance of the MLSE receiver operating at BER = 10^{-5}. As $|\Gamma|$ increases beyond 0.5 the losses become infinite for both receivers.

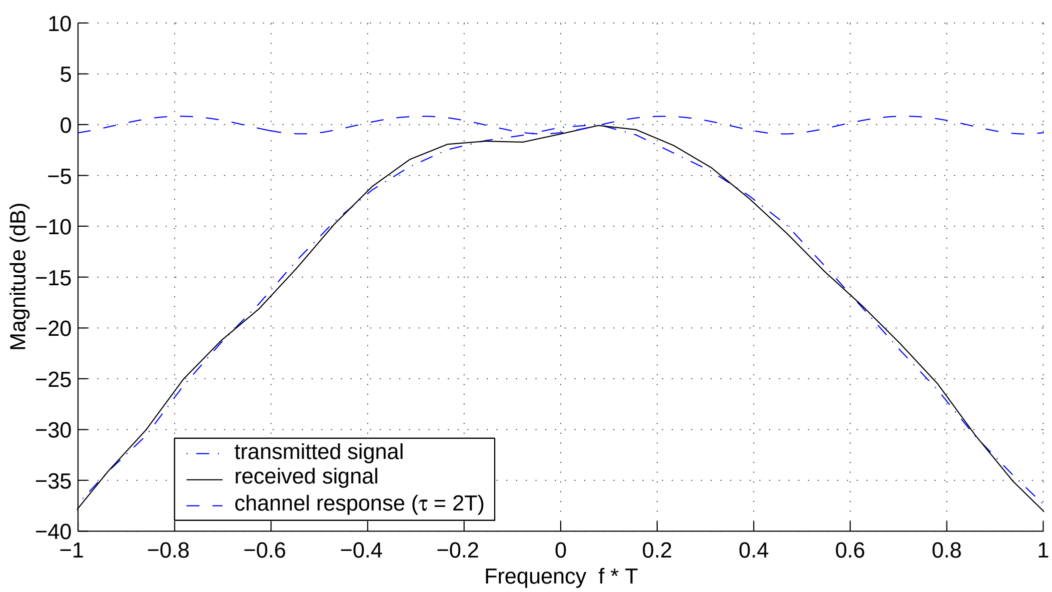

Figure 4: Comparison of multi-h CPM signal before and after passing through the weak-long channel. Channel parameters: $\Gamma = 0.1e^{j0.85\pi}$, $\tau = 2T$. Multi-h parameters: $M = 4$, 3RC with $h = \{4/16, 5/16\}$.

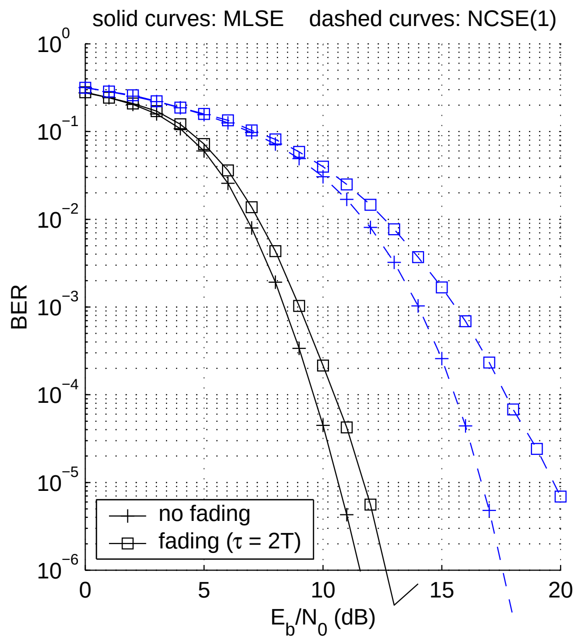

Figure 5: Performance of multi-h CPM using MLSE receiver over weak-long channel. The solid curves are for the MLSE receiver and the dashed curves are for the NCSE(1) receiver. The channel parameters are $\Gamma = 0.1e^{j0.85\pi}$ and $\tau = 2T$. At BER = 10^{-5} MLSE loses 1 dB in fading, and NCSE(1) loses 3 dB.